Presented at BIW04, Knoxville, May 3-6, 2004, AIP Conf. Proc. 732 (2004) pp. 244-8

Profile, Current and Halo Monitors of the PROSCAN Beam Lines

Rudolf Dölling

Paul Scherrer Institut (PSI), CH-5232 Villigen-PSI

Abstract. PROSCAN, an extended medical facility using proton beams for the treatment of deep seated tumours and eye melanoma, is under construction at PSI. Ionisation chambers and secondary emission monitors will be used as current monitors and in a multi-strip configuration as profile monitors at the PROSCAN beam lines. A thin and a thick version of these detectors are in preparation as well as a 4-segment ionisation chamber to detect the beam halo. Electromagnetic and microphonic noise from the signal and high-voltage cables, saturation due to recombination and the evaluation of the profiles are discussed as well as measures to detect failures of the detectors during operation.

INTRODUCTION

In the PROSCAN facility (Fig. 1) a 250 MeV proton beam of 1 to 500 nA will be extracted from the COMET cyclotron. After passing through a degrader, where the energy can be adjusted in the range from 230 to 70 MeV, it can be delivered, at a maximum current of 10 nA, into one of four areas: Two gantries, an eye treatment room and a material irradiation area. Fast changes of beam energy are foreseen for the spot-scanning treatment of deep-seated tumours in the new Gantry 2. Several diagnostics will be used to monitor the beam parameters in the various modes of operation (Fig. 1). The first components will be taken into operation this year.

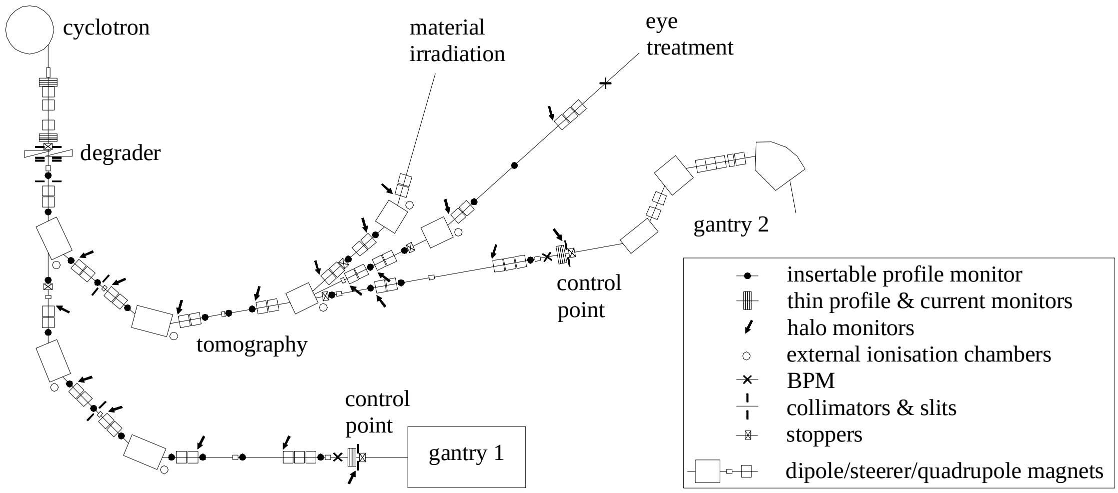

FIGURE 1. Overview of beam lines.

Presented at BIW04, Knoxville, May 3-6, 2004, AIP Conf. Proc. 732 (2004) pp. 244-8

THIN PROFILE MONITORS

In front of the degrader and at the "control point" in front of the gantries, profile and current monitors are inserted permanently in the beam. The current and their ratio are rapidly monitored as a safety measure. In addition, thin retractable monitors are available at the exit of the cyclotron. All these monitors must be very thin to prevent excessive scattering of the beam.

Planar ionisation chambers (IC) and multi-strip ionisation chambers (MSIC) filled with ambient air are used to obtain sufficient signal from the small beam currents (0.1 to 500 nA). These are formed by a stack of alternating high-voltage (HV) and measurement planes made from titanium foils of 6 μm thickness (Fig. 2). "1 broader + 30 regular + 1 broader"-strip patterns with 1 mm pitch are used for the measurement of (the projections of) the vertical and horizontal beam profiles. The two total-current measurements are used by the machine control system and by the patient safety system. Additional grounded foils are added at both sides of the stack to limit the active region and thereby decrease the maximum HV current load.

The pre-tensioned foils (full or with the etched strip pattern) are mounted on the supporting frames made from thick-film plated ceramic board. This is done by soldering, which requires a thin sputtered multi layer metal coating of the outer parts of the foil. The IC/MSIC measurement head is separated from the vacuum by a box with thin (25 or 50 μm) titanium windows, which are clamped between flanges.

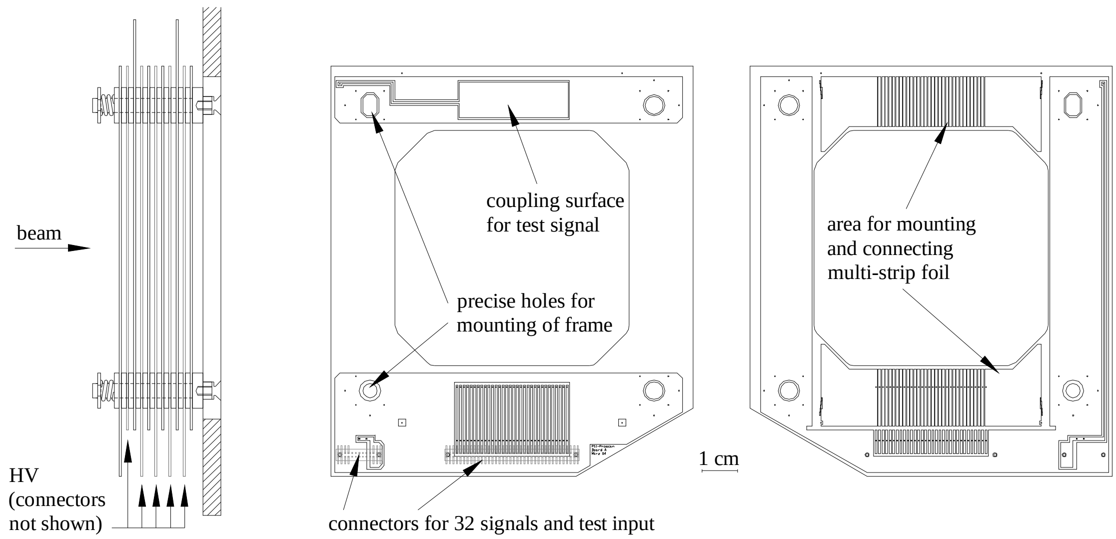

FIGURE 2. Left: Stack of frames with foils, forming 2 MSIC’s and 2 IC’s (vacuum enclosure and windows not shown). Middle and right: Supporting frame for multi-strip foil (front and back side).

At low beam currents recombination effects are negligible and the ratio “signal current/beam current” varies from 48 to 113 for proton energies of 250 to 70 MeV. With a gap of only 2 mm separating the planes and a bias of the HV-electrodes of +1.5 kV, the high electric field counteracts recombination and reduces the charge collection time t_{coll} = (plane separation)^2 * (high voltage)$^{-1}$ * (k_{air})$^{-1}$ to approximately 16 μs (with the mobility of air k_{air} ~$1.7{\cdot}10^{-4}$ m^2 s^{-1} V^{-1}). Nevertheless, with smaller beam diameters, recombination effects are dominant at higher beam currents (Fig. 3).

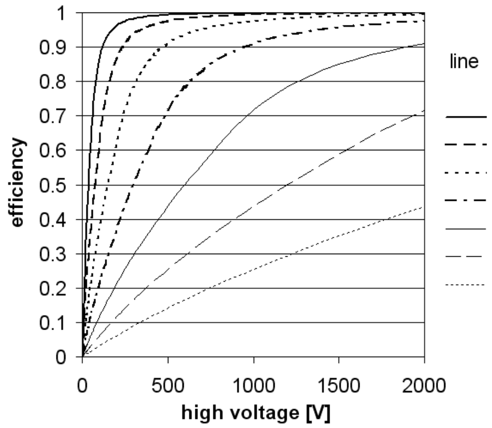

$\frac{(\text{beam current}[nA])(\text{gap}[mm])^4}{(\text{beam diameter}[mm])^2}$ @beam 250 MeV	beam diameter [mm] @beam 250 MeV, 512 nA and gap 2 mm or @beam 250 MeV, 32 nA and gap 4 mm or @beam 70 MeV, 13.6 nA and gap 4 mm
2	64
8	32
32	16
128	8
512	4
2048	2
8192	1

(round proton beam with homogeneous current density assumed)

FIGURE 3. Saturation of air filled ionisation chambers due to recombination (calculated according to [1]). The efficiency is a function of (plane separation)^4 * (beam current density) * (high voltage)$^{-2}$. Hence the curves can be scaled to other values of beam current, beam diameter, plane separation or high voltage than given in the right column of the legend.

In order to get signals not compromised by recombination, the same devices are placed in vacuum and used as multi-strip secondary emission monitors (MSSEM) and current monitors (SEM) at the locations near the cyclotron and in front of the degrader. Nevertheless, at low beam current the signal current, a few percent of the former, is too low for the electronics used. The stability of the secondary emission coefficient of titanium against ageing was one major reason for its choice [2].

INSERTABLE THICK PROFILE MONITORS

Insertable MSIC monitors, successively introduced into the beam by compressed-air actuators, yield the input information for the calculation of a beam envelope with the "Transport" code [3]. Since these monitors are not thin, only a measurement at one location at a time is possible. (As in the case of the thin monitors, the electronics used allow for the measurement of the temporal development of a beam profile.)

Metallised ceramic 0.63 mm thick boards separated by 4 mm wide air gaps provide the strip patterns and HV-electrodes. With one exception, a HV of +0.6 kV is sufficient to suppress the effect of recombination on the measured currents to below 10 % at the expected beam current densities and beam energies.

The strip pattern will be adjusted in the directions transversal to the beam to the requested accuracy of 0.1 mm to the reference given by the flange of the vacuum box.

The pitch of the metallised strips varies from 0.5 to 1 and 2 mm (plus one broader strip at each side). 2x 68 strips are fed out by flexible-printed-circuit cables.

With two exchangeable printed circuit boards placed in an electrically shielded box at the top of the profile-monitor feed-through, the signals are routed to the 2x 16 channels of the electronics. With this arrangement, a strip pitch of 0.5, 1, 1.5, 2, 3 or 4 mm can be chosen for a "1 broader + 14 regular + 1 broader"-strip arrangement in each plane (Fig. 4). This variability allows for the adaptation of the strip pitch to the expected range of beam profile width. This is required due to the limited number of only 16 channels per plane that is foreseen for most of the monitors.

At three successive locations, a higher resolution is foreseen for beam tomography. A "1 broader + 30 regular + 1 broader"-strip arrangement in each plane will be realised by doubling the number of cables and electronic modules. At these locations, the available strip pitch is 0.5, 1 or 2 mm.

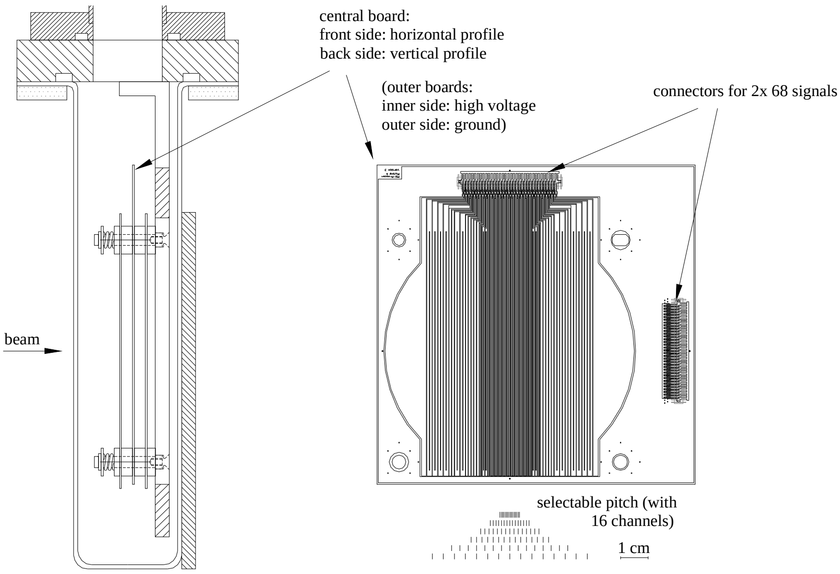

FIGURE 4. Insertable profile monitor.

PROFILE EVALUATION

The beam profile can be reconstructed from the measured currents to the strips by assuming a constant line-current density over the width of a strip. Nevertheless, in order to get a realistic representation of a broad beam profile in the region of the outer broader strips, it is required to combine the current readings from the outer broader strips with the information from the next inner strips (Fig. 5, [4]). This is essential for a correct determination of beam centre and beam width, which are evaluated from the first and second moments of the measured distribution. Without this technique, the width of broad beam profiles is usually overestimated.

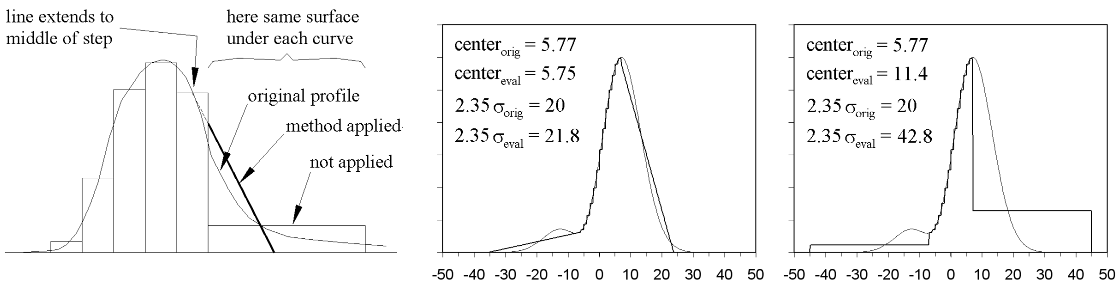

FIGURE 5. Treatment of broad beam profiles. Left: method, middle: applied to a fictitious profile, right: not applied. (Strip configuration: 1 strip from -45 to -7 units, 14 strips 1 unit wide from -7 to 7 units, 1 strip from 7 to 45 units. A precise current measurement without noise is assumed.)

For very narrow beams with a width comparable to or smaller than the strip pitch, the width is also usually overestimated. For beams with a width down to the strip pitch s_{pitch} this can be largely corrected by an empirical correction:

$$\sigma_{corr} = \sqrt{\sigma_{uncorr}^2 - 0.16\, s_{pitch}^2} \;.$$

Simulations [5] indicate that by a profile measurement using “1 + 14 + 1” strips beam position and width can be measured accurately when the FWHM beam width is in the range 1x to 10x strip pitch and the profile is of conventional shape. A pattern with varying strip pitch can also be chosen to further enlarge the range of beam profile width accessible with a fixed configuration.

HALO MONITORS

"Halo-monitors" are placed around modified bellows adjacent to the quadrupole doublets and triplets (Fig. 6). These 4-segment ionisation chambers, which protrude circumferentially 5 mm into the 90 mm diameter beam pipe, give enough signal to detect traversing beam current fractions of below 1 pA. This provides a much more sensitive loss control than the external ionisation chambers located near the dipole magnets and should also give an online control of the stability of the beam settings.

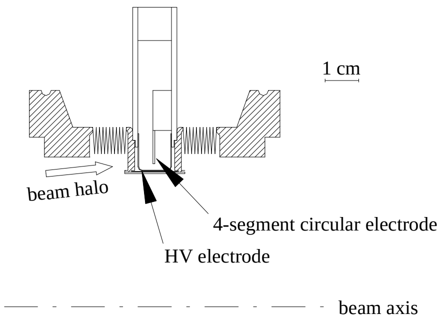

FIGURE 6. Halo monitor.

ELECTRONICS AND GROUNDING

With beam currents of 0.1 nA to 500 nA, the signal currents from MSIC, IC, MSSEM, SEM, Faraday-cups and halo monitors are of the order of 0.1 pA to 25 μA per single electrode. All currents are measured with multi-channel logarithmic-amplifier modules with a current range of 20 pA to >200 μA. These allow single channel readout as well as the measurement of up to 4096 profiles with a minimum time step of 1 ms. Algorithms for data evaluation and the generation of interlocks can be implemented. A trigger input allows the observation of time dependent machine behaviour by simultaneous operation of several modules [6]. The electronics, including the HV-modules for the detectors, are located some 40 meters away outside of the concrete shielding to prevent radiation damage and to allow for service without opening the bunker.

The very low signal levels require the elimination of ground loops. Therefore, the internal shield and "ground" of the analogue amplifier electronics is only grounded via the shield of the measurement-cable, which in turn is grounded at the diagnostic head at the beam line (Fig. 7). The ground of the digital electronics is connected to the (CAMAC- or VME-) crate ground. The ground transition for the signals is provided by a differential amplifier. Originally we intended to use this type of grounding for the HV-modules as well. However, locally grounded modules are now foreseen due to better availability.

CABLES, SHIELDING, NOISE AND FILTERS

In order to measure signal currents below 10 nA, it is imperative to use cables with a low production of microphonic noise and to prevent ground loops. Several cables have been tested for their susceptibility to microphonic noise and differences of several orders of magnitude were found. Ground loops are adequately prevented by the single point grounding scheme (see above) for the low frequencies of concern (<<300 kHz corresponding to $l_{\mathrm{cable}} \ll \lambda/30$). A good electrical shield is also of importance. The effectiveness of the cable shield against external AC electrical fields was also tested and large differences were found corresponding to the tightness of the shield.

A good standard in both aspects is the coaxial cable G03130HT, which is used for all single signals. It is a declared “low noise” cable using a semiconductor layer between the inner isolator and the dense copper braid. As signal cable for the MSIC and MSSEM, a 40 wire twisted-pair cable (Huber&Suhner No. 12 566 226) is used. A plastic coated aluminium tape and a copper braid (enclosing the whole bundle of 40 wires) give a compact shield. 32 wires carry the signals. The return path is provided by the cable shield and the residual wires (which as well could have been left floating). Hence no advantage is taken from the twisted pair property. This cable performes as well as the G03130HT. A similar cable with fewer wires (Huber&Suhner No. 12 568 329) is foreseen for the halo monitors. It should be noted that an individual shielding of each wire would give no advantage because the cross talk between the wires is already negligible due to the very low voltage burden of the electronics used.

Additional electrical shielding is provided by enclosing measurement- and HV-cables from each diagnostic head together in a second isolated shield (copper braid) which is grounded at many locations along the way. (With the HV-supplies grounded, it is disputable whether or not to include the HV-cable in this shield.) No attempts are made to magnetically shield the signal cables, but some efforts were made to separate the diagnostic cables from magnet, AC and stepping motor cables. Nevertheless, this was possible only to a limited degree due to boundary conditions from the infrastructure and concrete shielding. Furthermore, the diagnostic cables are placed on their own support, separate from water pipes, in order to reduce microphonic noise.

Grounding of both ends of the HV-supply cable causes a ground loop and noise is coupled to the HV-planes and from there capacitively to the signal electrodes. Hence, a filter for noise suppression is required (Fig 7., filter 1). The filter parameters are chosen to fulfill several requirements: A noise input voltage of 0.1 V to the cable (which is considered to be the worst case) should yield a noise signal below 1 pA, at least at frequencies above 50 Hz. With full signal, the high voltage should not drop below 90% of the zero-current value in order to preserve some stability against recombination. The slowing of the detector speed due to the "soft" high voltage must be moderate. I.e. 90% of the final value should be reached after approximately 10 µs (the charge collection time is not included in this number).

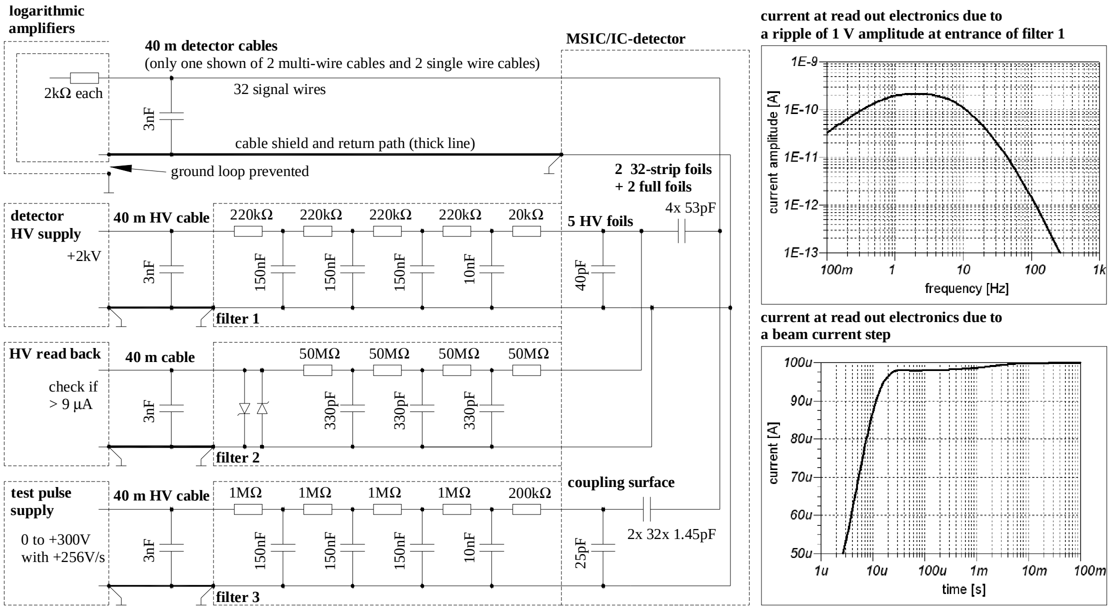

FIGURE 7. Filtering of HV input, HV read-back output (only one shown) and test-pulse input of the thin profile (MSIC) and current (IC) detector head. Detector and cable capacitances are roughly estimated. Also shown are cable shields and grounding. (With the given set-up, noise coupling to the HV read-back output and the test-pulse input is less critical than to the HV input.)

DETECTOR FAILURE SURVEILLANCE

In order to get the correct current reading from each electrode, it is required to have: intact foils in their correct position, high voltage at the HV-foils, signal path uninterrupted, signal path and signal foil isolated (i.e. not short circuited to ground or HV or other signal path), air present in IC's respectively vacuum in SEM's, intact current measurement electronics.

Possibilities for failures are:

- break of foil or solder joint (spontaneous or due to a break of a vacuum window) resulting in a misplacement or a loss of isolation or an interruption of the path to all or part of the signal
- bad connectors or break of PCB or wires resulting in interruption of the signal path
- humidity, radiation damage, sparking or sputter effects leading to a loss of isolation in the detector or in cables or connectors, resulting in an erroneous current reading or a loss of high voltage

- local disintegration of foils due to radiation damage or sparking or spark induced burning of foil (in air) which results - if the holes in the foil are larger than the gap between the planes - in too low current readings (“blind spot”)
- local change of the secondary emission coefficient of SEM planes (“blind spot”).

With all detectors, the mechanical integrity of the foils, the presence of the high voltage, the integrity of signal path and isolation and the readout electronics can be checked from time to time without beam: The high voltage is switched off and on with defined slopes, thereby capacitively inducing a signal to the measurement electrodes. This response can be compared to previously recorded data. The signal should be chosen small enough to detect even small leakage currents. Nevertheless, this method is hardly sensitive enough to detect e.g. a hole of a few mm diameter in a foil of 70 mm diameter or a break of the foil far from the readout-side.

The strip-foils can be checked in addition by capacitively coupling a test pulse (or AC voltage) only to the end of the strips opposite to the readout-side (Figs. 2, 7). The set-up from Fig. 7 results in a pulse of 210 pA height and 1.7 s FWHM.

At the safety relevant current monitors, the presence of the high voltage at all electrodes is checked online. The high voltage is provided to one electrode and via a chain of connectors to the other HV-electrodes. From the last HV-electrode, the potential is fed back to the read-out electronics which is part of the patient-safety system. (An additional read-out is provided to the machine control system.) This feedback is filtered so that any retroaction of the readout electronics to the high voltage at the HV-electrode is negligible.

As a further control, the total currents (with beam) of the individual measurement planes can be compared. This is the only available means to detect small holes in the foils. (It is assumed that a larger fraction of the beam passes through the hole and that holes in different planes are not formed at the same time.) At the same time the readout electronics are checked against each other. This check should be performed regularly.

In the same way a change of the secondary emission coefficient can be detected by comparing the output of SEM’s and IC’s.

REFERENCES

1. Mie, G., „Der elektrische Strom in ionisierter Luft in einem ebenen Kondensator“, *Ann. Phys. (Leipzig)* **13,** 857-889 (1904). See also: H. Attix, “Boag’s treatment of Mie’s theory” in *Introduction to radiological physics and radiation dosimetry*, Wiley, 1986, pp. 334-336.
2. Ferioli, G., and Jung, R., “Evolution of the secondary emission efficiencies of various materials measured in the CERN SPS secondary beam lines”, DIPAC’97, 1997, pp. 168-170.
3. http://people.web.psi.ch/rohrer_u/trans.htm.
4. Dölling, R., „Methode der Auswertung von MSIC-Messungen“, PROSCAN-document P24/DR84-401 (2004).
5. Dölling, R., „Auswertung von MSIC-Messungen und Einfluss der Streifenzahl auf die Genauigkeit von Profilschwerpunkt und –breite“, PROSCAN-document P24/DR84-305 (2003).
6. Duperrex, P.-A., et al., these proceedings.
7. Dölling, R., „Messkabel für kleine Ströme bei der Strahlführungsdiagnostik PROSCAN“, PROSCAN-document P24/DR84-403 (2004).